Visual Neuroscience (1999), **16**, 107–120. Printed in the USA.
Copyright © 1999 Cambridge University Press 0952-5238/99 $12.50

Morphology of wide-field, monostratified ganglion cells of the human retina

BETH B. PETERSON AND DENNIS M. DACEY

Department of Biological Structure, The University of Washington, Seattle

(RECEIVED March 2, 1998; ACCEPTED June 22, 1998)

Abstract

To determine the number of wide-field, monostratified ganglion cell classes present in the human retina, we analyzed a large sample of ganglion cells by intracellular staining in an *in vitro*, whole-mount preparation of the retina. Over 1000 cells were labeled by horseradish peroxidase or Neurobiotin; some 200 cells had wide dendritic trees narrowly or broadly stratified within either the inner (ON) or outer (OFF) portion of the inner plexiform layer. Based on dendritic-field size and the pattern and extent of dendritic branching, we have distinguished six wide-field cell groups. The giant very sparse ganglion cells included both inner and outer stratifying cells and were unique both for their extremely large dendritic field (mean diameter = 1077 μm) and extremely sparsely branched dendrites. Four of the cell groups had similarly large dendritic fields, ranging in mean diameter from 737 to 791 μm, but differed in the pattern and extent of dendritic branching, with the number of dendritic branch points ranging from a mean of 33 to 129. Of these four groups, the large very sparse group and the large dense group included both inner and outer stratifying cells, while the large sparse and large moderate groups consisted of inner stratifying cells only. The thorny monostratified ganglion cells were distinct from the other cells in having medium size dendritic fields (mean diameter = 517 μm) and moderately branched, inner stratifying dendritic trees with many thin, spiny, twig-like branchlets. All six groups had medium-size cell bodies, with mean soma diameters ranging from 17 to 21 μm. Though the physiological properties and central projections of human wide-field, monostratified ganglion cells are not known, some of the cells resemble macaque ganglion cells known to project to the lateral geniculate nucleus, the pretectum, or the superior colliculus.

Keywords: Human retina, Ganglion cell types

Introduction

Since Cajal first demonstrated over 100 years ago that the vertebrate retina contains a great morphological diversity of ganglion cells (Ramon y Cajal, 1893), the number of functionally distinct ganglion cell types has been the focus of continued study. In primate retina, the morphology, physiology, and central projections of the two major classes of ganglion cells, the parasol and midget cells, have been well studied (Boycott & Dowling, 1969; Leventhal et al., 1981, 1993; Perry et al., 1984; Watanabe & Rodieck, 1989; Dacey & Petersen, 1992; Silveira et al., 1994; Ghosh et al., 1996; Yamada et al., 1996). A third type of ganglion cell, the small bistratified cell, has also been well characterized (Rodieck & Watanabe, 1993; Dacey, 1993; Dacey & Lee, 1994; Ghosh et al., 1996). The parasol, midget, and small bistratified ganglion cells transmit luminance and color related signals to primary visual cortex *via* the lateral geniculate nucleus (LGN). These three pathways are important for visual perception (Dacey, 1994, 1996), yet it is now clear that they represent only a small fraction of the number of ganglion cell types that project to the LGN and to midbrain targets. For example, Hendry and Yoshioka (1994) have shown that cells in the interlaminar zones of macaque LGN immunoreactive for type II calmodulin-dependent kinase provide input to the cytochrome oxidase-rich blobs in primary visual cortex, and Rodieck and Watanabe (1993) retrogradely labelled a population of large-field, monostratified ganglion cells following tracer injection into the parvocellular layers of macaque LGN. Retrograde labelling following tracer injection into the superior colliculus and pretectum of macaque monkeys (Leventhal et al., 1981; Perry & Cowey, 1984; Rodieck & Watanabe, 1993) has revealed a diversity of large-field ganglion cell types that project to these regions of the midbrain.

Golgi studies of human retina (Kolb et al., 1992) have suggested that there may be as many as 20 different types of ganglion cells subserving the various pathways of parallel processing in the visual system, yet to date there have been no quantitative studies of the number of ganglion cell types. As a first step towards determining the number of ganglion cell types in the human retina, we are analyzing a large sample of ganglion cells intracellularly filled with either horseradish peroxidase (HRP) or Neurobiotin (Dacey et al., 1991; Dacey & Petersen, 1992; Dacey, 1993; Peterson & Dacey, 1998). In the present study, we show that there are

Correspondence and reprint requests to: Dennis M. Dacey, Department of Biological Structure, HSC G514, Box 357420, The University of Washington, Seattle, WA 98195-7420, USA.

at least six distinct groups of wide-field, monostratified ganglion cells in human retina. Based on morphological comparisons with studies in macaque, we suggest that some of these cells may represent human correlates of wide-field, monostratified macaque ganglion cells that project to the LGN, the pretectum, or the superior colliculus.

Materials and methods

In vitro intracellular injection and histology in the isolated retina

The *in vitro* retinal whole-mount preparation and intracellular injection technique have been previously described (Dacey & Petersen, 1992; Dacey, 1993). Human eyes ($n = 46$, age range 16–82 years) were obtained 90–120 min after death from donors to the Lions Eye Bank at the University of Washington. In brief, the retina was dissected free of the sclera and choroid in continuously oxygenated culture medium (Ames, Sigma Chemical Co., St. Louis, MO) and placed flat in a superfusion chamber on the stage of a light microscope, with no apparent deterioration in morphology of cells maintained in the chamber for ~8–10 h.

Ganglion cells were observed under episcopic illumination following *in vitro* staining with acridine orange. Intracellular injections were made into fluorescing cells with electrodes filled with Lucifer yellow (~2%; Aldrich Chemical, Milwaukee, WI) in 20 mM, pH 7.0 MOPS buffer (Sigma Chemical Co., St Louis, MO) and either rhodamine-conjugated horseradish peroxidase (HRP) (~4%; Sigma Chemical Co., St Louis, MO) or Neurobiotin (~4%; Vector Labs, Burlingame, CA). Lucifer yellow fluorescence in the electrode and acridine orange fluorescence of ganglion cells were observed with the same excitation filter (410–490 nm; barrier filter 515 nm), permitting direct observation of the electrode tip as it penetrated a cell. Successful penetration was confirmed by passing Lucifer yellow into an impaled cell. Ganglion cells were then filled with either rhodamine-conjugated HRP or Neurobiotin.

Following an experiment, retinas were fixed for 2–3 h in phosphate-buffered fixative (2% glutaraldehyde, 2% paraformaldehyde, or 4% paraformaldehyde; 0.1 M, pH 7.4). Cells injected with rhodamine-conjugated HRP were revealed using diaminobenzidine (DAB) as the chromogen. Retinas were incubated in the DAB solution (0.1% in 0.1 M phosphate buffer, pH 7.4) for 5 min, then H_2O_2 (0.003%) was added and the retinas further incubated for 3–4 min. Retinas were rinsed in buffer, wholemounted on gelatin-coated slides, air dried, then dehydrated in a graded alcohol series, cleared in xylene, and coverslipped.

Neurobiotin injected cells were revealed by HRP histochemistry using the Vector ABC protocol (Vector, Elite kit). Retinas fixed in 4% paraformaldehyde were placed in 0.5% tritonX-100 (0.1 M phosphate buffer, pH 7.4) for 3 h at room temperature, then incubated in buffer containing the Vector avidin-biotin-HRP complex for 3 h. The retinas were rinsed in buffer for 1 h before performing standard HRP histochemistry using DAB as the chromogen as described above.

Data analysis

The location of every injected ganglion cell relative to the foveal center was recorded for each retina. A camera-lucida tracing of the dendritic tree (total magnification, 480×) and an outline of the cell body (total magnification, 1940×) were made for each cell. Dendritic-field area was determined by tracing a convex polygon around the perimeter of the traced dendritic tree and entering the outline into a computer *via* a graphics tablet. Dendritic-field diameter was expressed as the diameter of a circle with the same area as that of the polygon. Similarly, cell body size was expressed in terms of an equivalent diameter.

The extent of dendritic branching was quantified as "number of branch points" by counting the terminations of the dendritic branches of the cells in the camera-lucida tracings. Branch point counts were made by one individual and verified by a second individual prior to cell classification. Some of the cells were notable for the presence of many fine dendritic spines and twig-like branchlets, raising the question of which dendritic processes should be counted as branches. We used the criterion that a process must be greater than 10 μm in length to be counted as a dendritic branch. This criterion was based on our observation that in ganglion cells where there are no "branchlets" and where dendritic branches can be unambiguously distinguished from dendritic spines, the longest spines measured were very fine caliber processes 6–7 μm in length.

Dendritic stratification in the inner plexiform layer (IPL) was determined by taking measurements with reference to the ganglion cell layer border and inner nuclear layer border at several locations in the dendritic tree. Stratification is described as being in the inner or outer half of the IPL without a more precise determination of the depth of stratification. The reason for this is that whereas shrinkage in the plane of the retina was minimal (~2%), we estimate about a 60–70% vertical shrinkage in our preparations as a result of tissue processing. At the eccentricities of the cells in the present study, the thickness of the IPL ranged from about 9 μm near the midperiphery to about 4 μm in the far periphery, making it impossible to measure with reasonable accuracy the exact depth of stratification with the 1-μm scale of the microscope's fine focus knob.

Results

Identification of ganglion cell groups

The cells in this study came from a sample of over 1000 intracellularly injected human retinal ganglion cells containing a diversity of morphological types (Dacey et al., 1991). Within this larger sample, we found a heterogeneous group of 203 wide-field, monostratified ganglion cells. Fig. 1 shows the wide-field cells plotted for dendritic-field diameter as a function of eccentricity along with data on parasol and midget ganglion cells from a previous study (Dacey & Petersen, 1992) for comparison. The wide-field cells formed a cluster distinct from the two other major classes of monostratified ganglion cells. Nineteen of the wide-field cells had a distinctive morphology that included axonal branching and short, terminal axon collaterals as described in a previous report (Peterson & Dacey, 1998) and are not discussed here. The remaining 184 wide-field cells differed somewhat in dendritic-field size but showed a greater diversity in the extent and pattern of dendritic branching, suggesting they represented multiple cell types. To unequivocally determine the number of discrete types represented by the wide-field cells, information as to their distribution in the ganglion cell layer and the mosaics they form would be necessary. This was not possible in the present study where only a few to at most a dozen cells were randomly filled in each of 29 retinas.

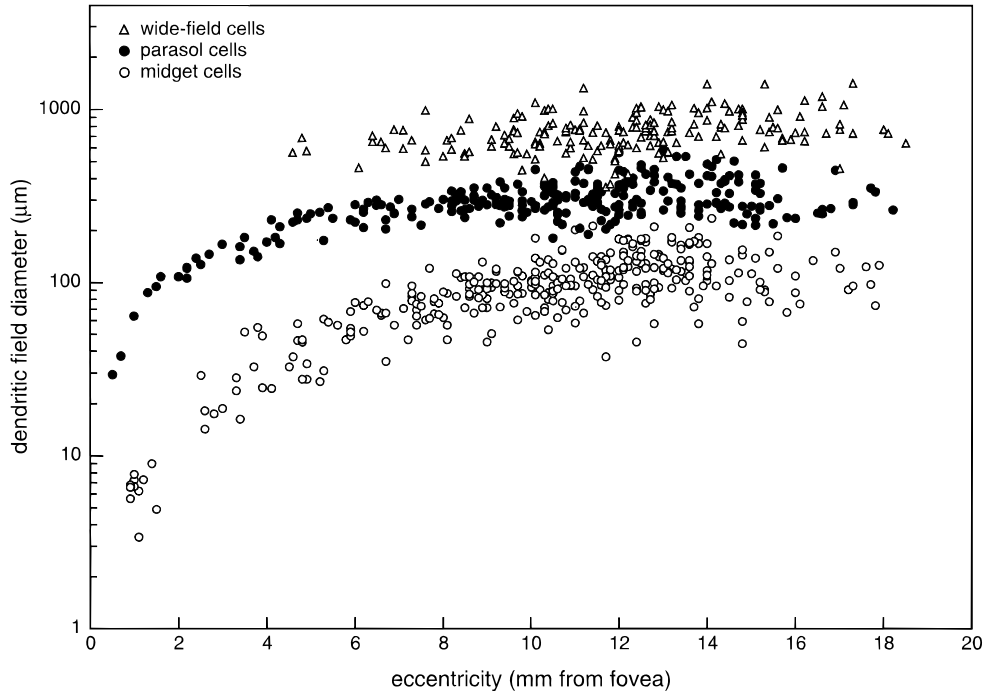

Fig. 1. Dendritic-field diameters of wide-field, parasol, and midget ganglion cells of the human retina plotted as a function of distance from the fovea. Wide-field cells formed a cluster distinct from the other two major classes of monostratified ganglion cells.

Given the limitations of the present study, our approach was to classify the wide-field cells into broad groups as determined by measurable morphological characteristics and obvious differences in patterns of dendritic branching. We used scatter plots to analyze the cells on the basis of dendritic-field size, number of dendritic branches, and eccentricity (Fig. 2). The majority of cells were similar in dendritic-field size, though there was a scattering of cells with larger and smaller dendritic fields (Fig. 2A). The cells showed a wide range in the extent of dendritic branching, with some cell densities apparent in the lower and middle branch point range (Fig. 2B). When dendritic-field size was plotted as a function of branch point number (Fig. 2C), cell densities were more pronounced and some patterns became clearer. For example, cells with the largest dendritic fields tended to have the sparsest branching dendritic trees whereas cells with the smallest dendritic fields fell into a midrange for dendritic branching. When all three parameters shown in Fig. 2 were plotted simultaneously in a three-dimensional space, clear clustering became apparent and we found that 179 of the cells fell into six groups which we have termed giant very sparse, large very sparse, large sparse, large moderate, large dense, and thorny monostratified. Three of the six groups were further divided into inner (ON) and outer (OFF) cells based on stratification in the IPL. Five of the cells shown in Fig. 2 did not fit into any of these groups and were designated "others" as discussed below.

Giant very sparse cell group

The giant very sparse group formed a cluster of 10 cells in the three-dimensional scatter plot of Fig. 3. The two-dimensional plots of Figs. 2A, 2B, and 2C comprise the three planes of Fig. 3, with each cell represented by a data point in three-dimensional space as determined by its dendritic-field diameter, number of dendritic branch points, and eccentricity. The orientation of the plots in Figs. 3, 6, and 9 are similar and were chosen to allow the best view of clustering in the branch point number/dendritic-field diameter and branch point number/eccentricity planes. None of the plots compensates for the asymmetric distribution of ganglion cells in the retina. Our sample included cells from all four retinal quadrants, yet we found no marked differences in dendritic-field diameter or branch point number when nasal cells were plotted separate from the other cells (not shown).

Giant very sparse cells had exceptionally large dendritic trees (Figs. 3 and 4A) with a mean dendritic-field diameter several hundreds of microns larger than any of the other groups (Table 1). The cells were the most sparsely branched of the wide-field cells (Fig. 3 and Table 1), with typically thick, somewhat spiny, straight-projecting dendrites (Figs. 4A and 5A). In seven of these very large cells, including the one shown in Fig. 4A, some of the dendrites thinned and faded at their tips, indicating incomplete fills. The mean dendritic-field diameter for this group, therefore, may be somewhat larger than our calculations. Giant very sparse cells had medium-size cell bodies, as did all the cells in this study (Table 1), and consisted of both inner and outer stratifying cells. Axons were thin ($\sim$2 μm) and usually originated from the soma (arrow in Fig. 4A) though the axons of a few cells appeared to originate from a secondary dendrite (arrow in Fig. 5A). Giant very sparse cells showed a trend towards increasing dendritic field size with increasing eccentricity but no trend in branch point number or soma size with eccentricity (not shown).

Although most of the cells in this study were filled with HRP, a small number of cells, including the cell in Fig. 5A, were filled

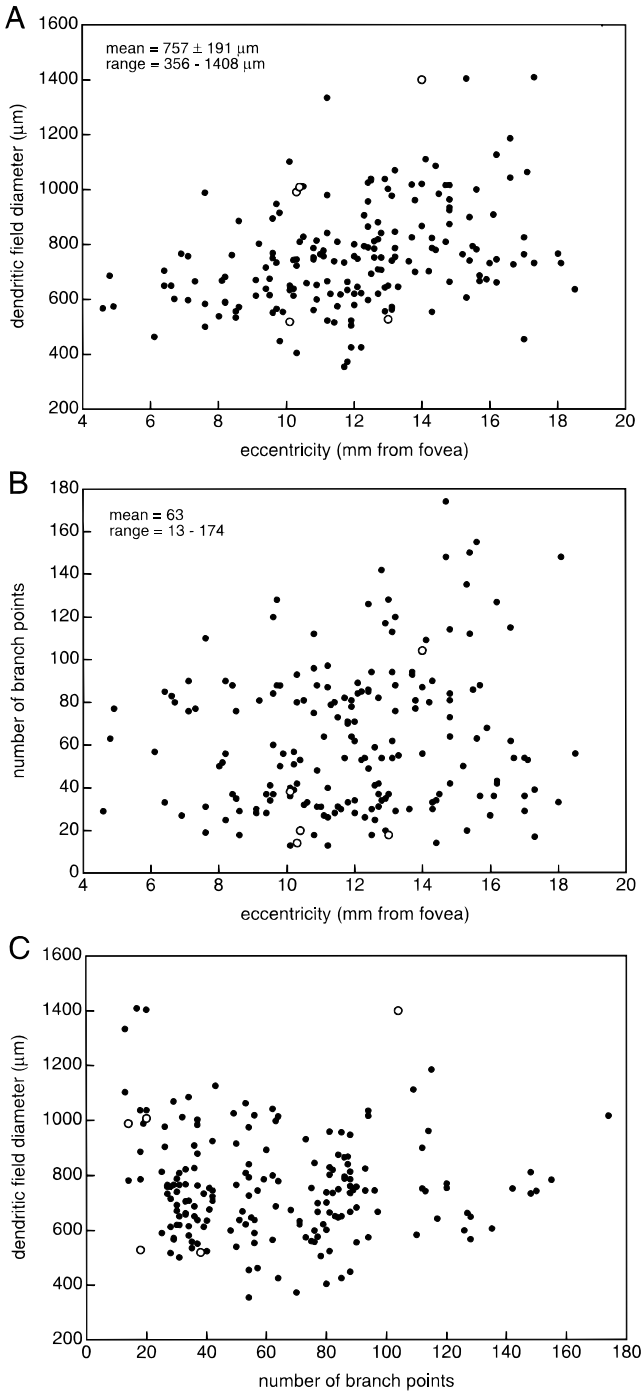

Fig. 2. Scatter plots of 184 wide-field, monostratified ganglion cells. (A) The majority of cells formed a single cluster when plotted for dendritic-field size as a function of eccentricity, with some scattering of cells with larger and smaller dendritic fields. (B) Cells showed a wide range in the extent of dendritic branching when plotted for branch point number versus eccentricity. Some cell densities in the lower and middle ranges of branch point number can be seen but there is no apparent clustering. (C) When plotted for dendritic-field diameter as a function of branch point number, cell densities were more pronounced and some patterns became more obvious. Note that cells with the largest dendritic fields tended to have the sparsest branching dendritic trees and cells with the smallest dendritic fields fell in the middle range for branch point number. Closed symbols (●) denote cells shown in the three-dimensional scatter plots of Figs. 3, 6, and 9. Open symbols (○) denote the five cells described in the text as "others."

with Neurobiotin. Because of its small size, Neurobiotin can show tracer coupling between cells of the same type (homotypic coupling) or of different types (heterotypic coupling) when such cells are coupled through gap junctions. The arrowhead in Fig. 5A shows the stained soma of an amacrine cell which appeared to be coupled to this giant very sparse ganglion cell.

Large very sparse, large sparse, large moderate, and large dense cell groups

The large very sparse, large sparse, large moderate, and large dense monostratified ganglion cells were similar in dendritic-field size and soma size (Table 1). They differed in the extent of dendritic branching, as shown in the scatter plots of Figs. 3 and 6, where the cells formed four distinct clusters. The large sparse and large moderate cells are also shown in the plot of Fig. 9 for comparison with the thorny monostratified ganglion cells described below.

Large very sparse cells formed a cluster of 58 cells (Fig. 3). They generally had somewhat thick, spiny dendrites that projected straight from the cell body with a simple branching pattern (Figs. 4B and 5B). There was some variability in the spiny appearance and thickness of the dendrites, and some dendrites of a few cells showed some retroflexive branching. Large very sparse cells had thin axons (~2 μm) that originated either from the soma (arrow in Fig. 5B), from a primary (arrow in Fig. 4B), or from a secondary dendrite. The large very sparse group consisted of both inner and outer stratifying cells (Table 1). Of the eight Neurobiotin-filled cells in the large very sparse group, two inner and one outer stratifying cell showed coupling to what appeared to be a single type of small-bodied amacrine cell. Large very sparse cells showed a trend towards increasing dendritic-field size with increasing eccentricity, but no trend in branch point number or soma size with eccentricity (not shown).

The large sparse group consisted of 27 inner stratifying cells (Figs. 3, 6, 9, and Table 1). No outer stratifying cells were seen in this group. The cells had a similar morphology with somewhat thick and fairly spiny dendrites that projected in a simple, straight pattern from the soma (Figs. 7A and 8A). Axons were thin (~2 μm) and originated from the soma (arrows in Figs. 7A and 8A) or, in a few cases, from a primary dendrite. Large sparse cells showed an increase in dendritic-field size with increasing eccentricity, but no change in either soma size or branch point number with eccentricity (not shown).

Large sparse and large very sparse cells were very similar in their simple, radiate pattern of dendritic branching (compare Figs. 7A and 4B), making it sometimes difficult to differentiate the cells in these two groups based solely on a subjective judgement of their appearance. For example, a sparsely branching cell with a large dendritic tree will look more "sparse" than a smaller cell with the same number of branches. The large sparse and large very sparse groups differed primarily in the extent of dendritic branching, forming distinct, nonoverlapping clusters in the plot of Fig. 3. Also, the large very sparse group included both inner and outer stratifying cells whereas we found no outer stratifying cells in the large sparse group (Table 1).

The large moderate group consisted of 48 inner stratifying cells. As with the large sparse cells, no outer stratifying cells were seen in this group. The plots of Figs. 6 and 9 show large moderate cells forming a discrete cluster that does not overlap the large sparse or large dense cell groups. Large moderate cells had a similar dendritic morphology as typified by the cell shown in Fig. 7B. Den-

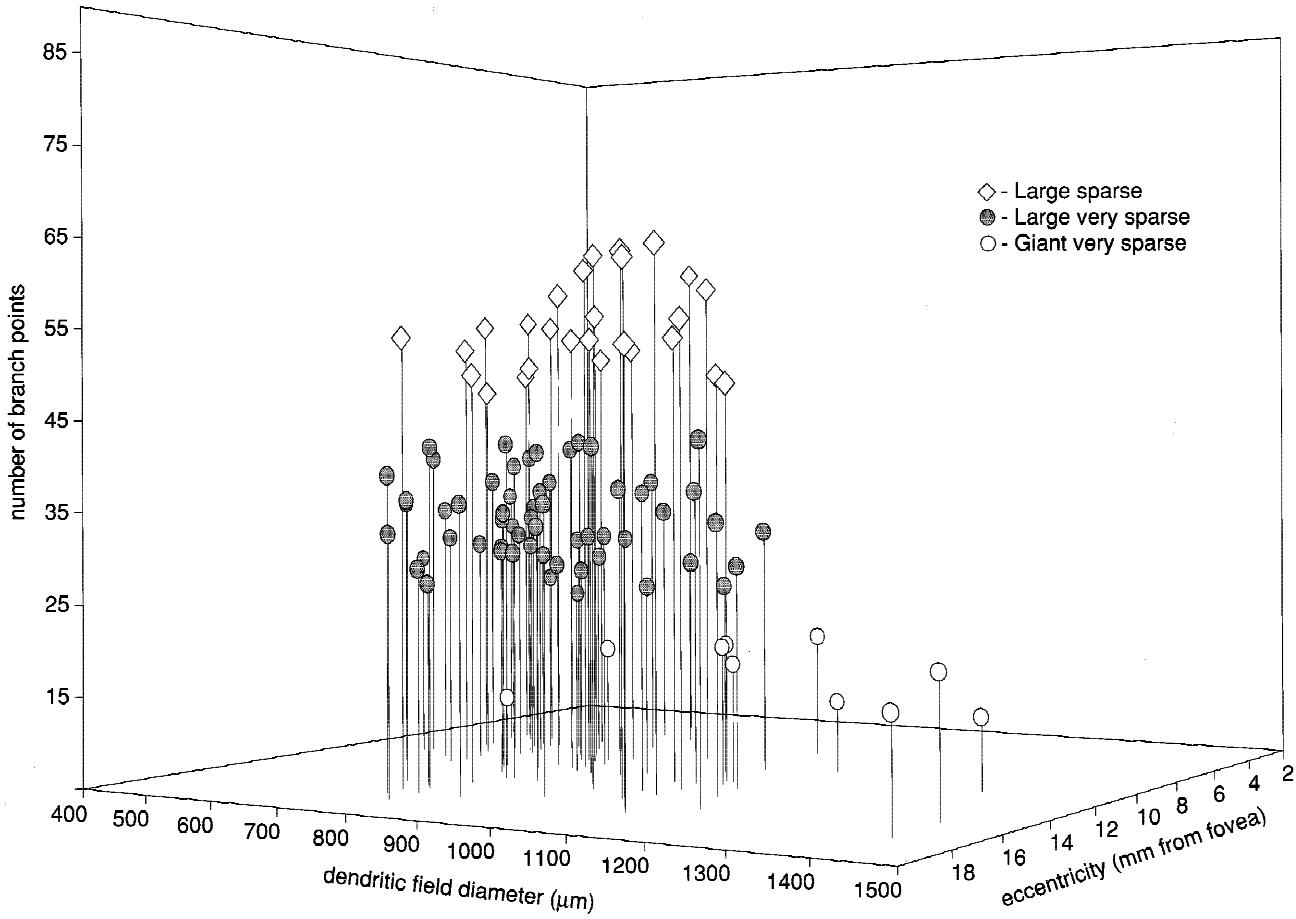

Fig. 3. Three-dimensional scatter plot of wide-field, monostratified ganglion cells plotted by dendritic branch point number as a function of dendritic-field diameter and eccentricity. Cells formed nonoverlapping clusters. Large sparse and large very sparse cells were similar in dendritic-field size but differed in the extent of dendritic branching. Giant very sparse cells had the largest and most sparsely branched dendritic trees. Large sparse cells are also shown in the plots of Figs. 6 and 9.

Table 1. *Wide-field monostratified ganglion cells of the human retina*

Cell group	Sample size	Eccentricity range (mm from fovea)	Mean dendritic field diameter (μm ± S.D.)	Range (μm)	Mean soma diameter (μm ± S.D.)	Range (μm)	Mean number of branch points (±S.D.)	Range
Giant very sparse—inner	5	8.6–15.3	1090 ± 271.1	787–1404	19 ± 2.7	16–22	18 ± 2.9	13–20
Giant very sparse—outer	5	7.6–17.3	1064 ± 227.1	781–1408	23 ± 5.0	16–28	16 ± 2.6	13–19
Total	10	7.6–17.3	1077 ± 236.2	781–1408	21 ± 4.5	16–28	17 ± 2.7	13–20
Large very sparse—inner	44	6.4–18.0	715 ± 141.8	501–1129	20 ± 3.5	13–29	35 ± 4.6	25–43
Large very sparse—outer	14	4.6–14.8	807 ± 160.3	517–1069	19 ± 4.2	15–30	29 ± 4.3	25–42
Total	58	4.6–18.0	737 ± 150.4	501–1129	20 ± 3.7	13–30	33 ± 5.0	25–43
Large sparse[a]	27	4.8–17.1	791 ± 174.0	463–1062	18 ± 3.6	13–28	56 ± 4.9	48–64
Large moderate[a]	48	4.9–15.5	749 ± 126.6	523–1034	18 ± 2.7	13–26	84 ± 6.7	71–97
Large dense—inner	17	7.6–16.6	793 ± 184.3	567–1186	19 ± 3.0	14–26	127 ± 18.5	109–174
Large dense—outer	4	12.9–18.1	712 ± 76.2	643–811	16 ± 1.3	15–18	135 ± 15.6	117–148
Total	21	7.6–18.1	777 ± 170.6	567–1186	18 ± 2.9	14–26	129 ± 17.9	109–174
Thorny[a]	15	8.5–18.5	517 ± 112.7	356–674	17 ± 2.2	15–21	70 ± 12.5	54–88

[a]These are inner stratifying cells only.

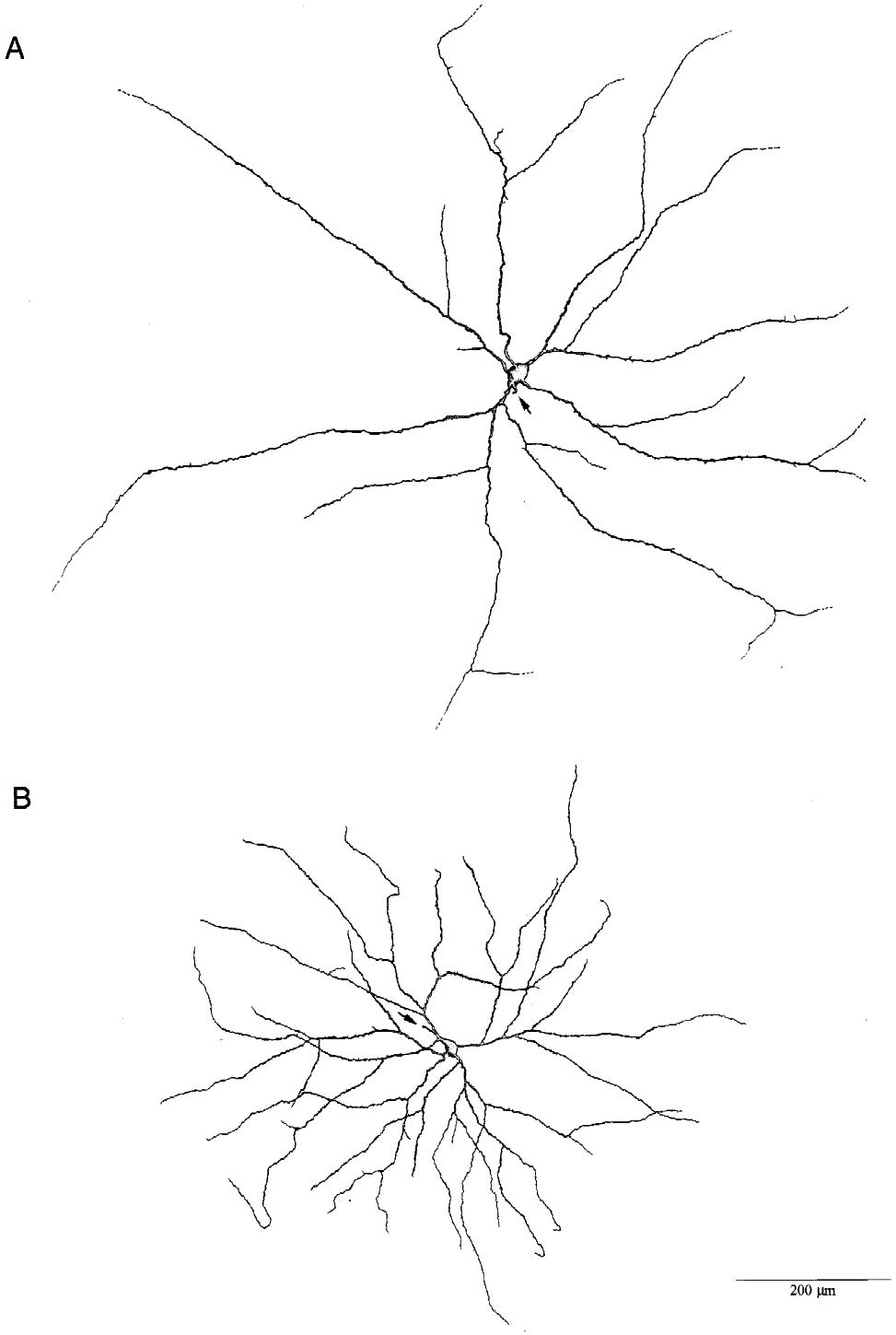

Fig. 4. Camera-lucida tracings of two HRP-filled wide-field, monostratified ganglion cells. Axons are indicated by arrows. (A) Outer stratifying giant very sparse ganglion cell located in lower retina 7.6 mm from the fovea. The cell had a dendritic-field diameter of 989 μm, soma diameter of 27 μm, and 19 branch points. (B) Inner stratifying large very sparse ganglion cell from lower retina, eccentricity 6.4 mm. Dendritic-field diameter was 705 μm, soma diameter was 21 μm, and the cell had 33 branch points.

drites were spiny and initially somewhat thick but tapered over their length and gave rise to thinner terminal branches that filled in the dendritic field more densely than the large sparse cells. The photomicrograph of Fig. 8B is of the same cell shown in Fig. 7B. Large moderate cells had thin axons ($\sim$2 μm) that originated either from the soma or from a primary dendrite (arrows in Figs. 7B and 8B). Cells in the large moderate group showed a slight trend towards increasing dendritic-field diameter with increasing eccentricity and no change in branch point number or soma size with eccentricity (not shown).

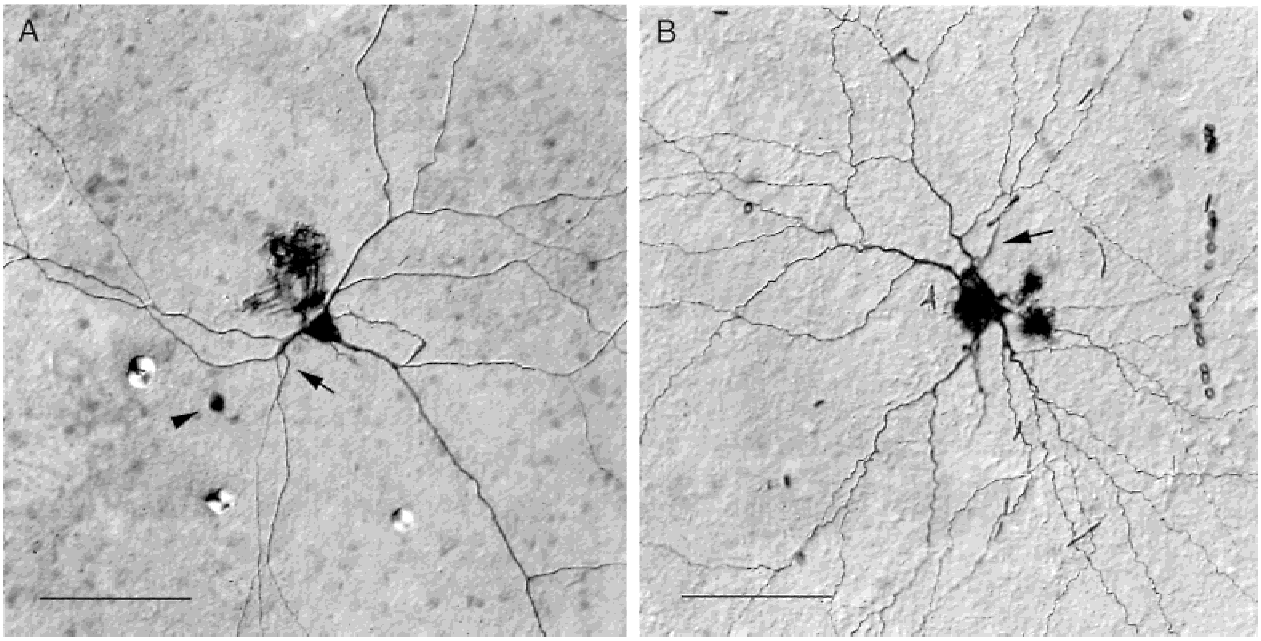

Fig. 5. Photomicrographs of Neurobiotin- and HRP-filled wide-field, monostratified ganglion cells. Axons are indicated by arrows. (A) Inner stratifying giant very sparse ganglion cell from lower retina, eccentricity 12.9 mm. The cell had a large dendritic tree (diameter = 1037 μm) with only 20 branch points. Soma diameter was 21 μm. Some glial cell processes near the cell body have been stained. Arrowhead indicates the small soma of an amacrine cell coupled to this Neurobiotin-filled ganglion cell. (B) Outer stratifying large very sparse ganglion cell from lower retina, eccentricity 14.8 mm. The cell had a dendritic-field diameter of 925 μm and 42 branch points. The unusually large soma (diameter = 30 μm) is partially obscured by stained glial cell processes. Scale bars = 100 μm.

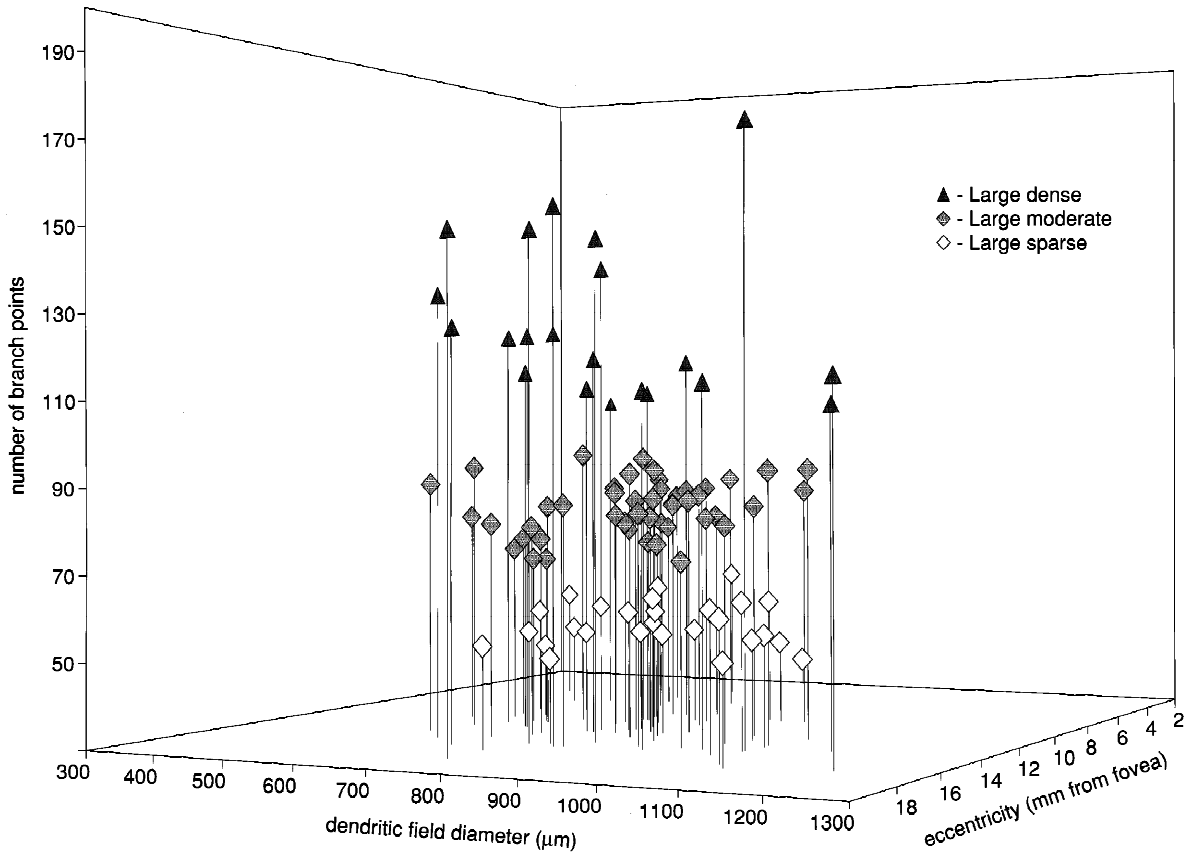

Fig. 6. Three-dimensional scatter plot of wide-field, monostratified ganglion cells. The large dense, large moderate, and large sparse cells formed three nonoverlapping clusters when plotted by dendritic branch point number as a function of dendritic-field diameter and eccentricity. The large moderate and large sparse cells are also shown in the plot of Fig. 9.

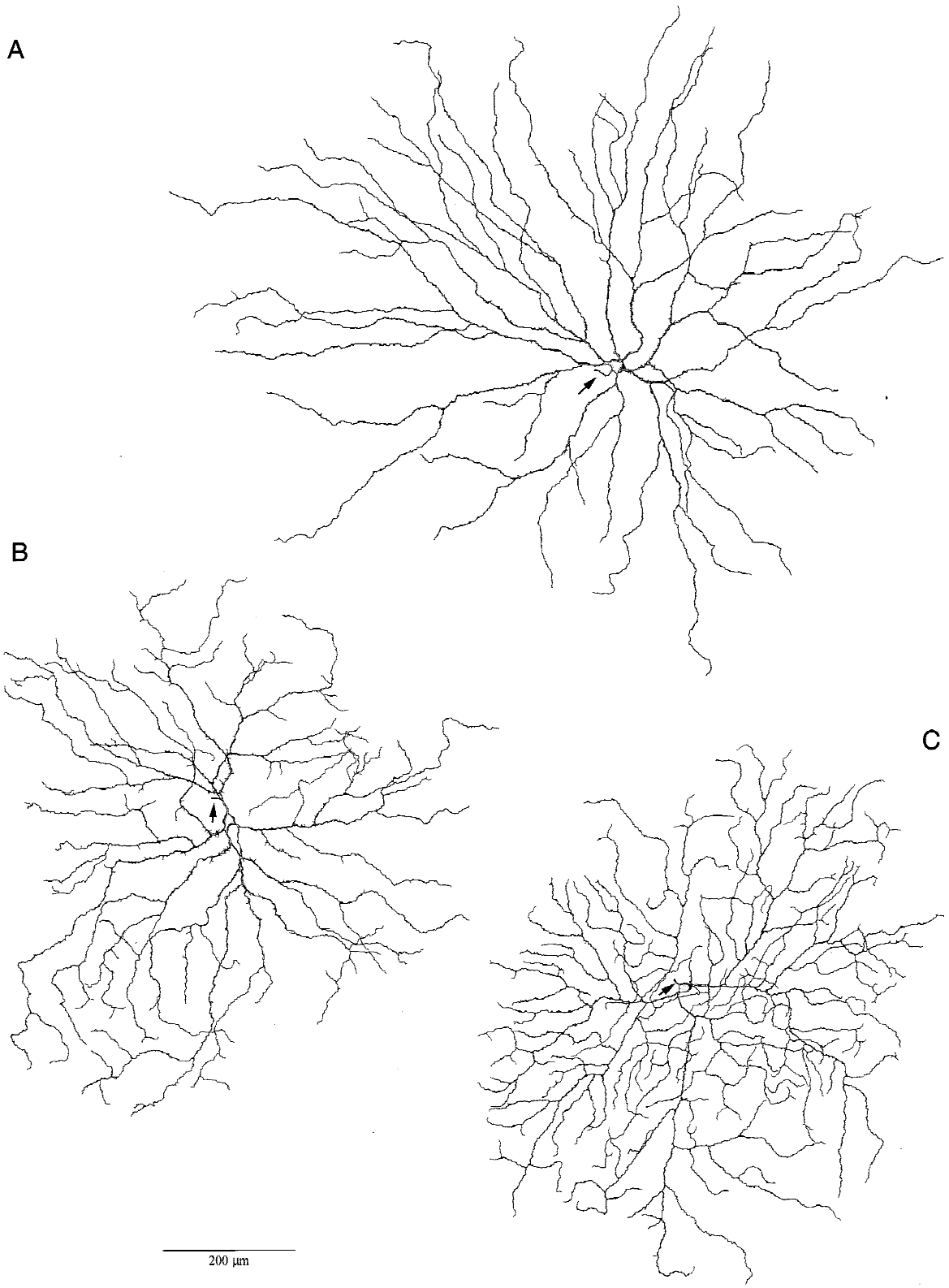

Fig. 7. Camera-lucida tracings of three HRP-filled wide-field, monostratified ganglion cells. Axons are indicated by arrows. (A) Inner stratifying large sparse ganglion cell from nasal retina, eccentricity 13.1 mm. This cell had a very large dendritic tree 976 μm in diameter with 54 branch points. Soma diameter was 22 μm. (B) Inner stratifying large moderate ganglion cell from upper retina, eccentricity 7.1 mm. Soma diameter was 18 μm, dendritic-field diameter was 759 μm, and the cell had 90 branch points. (C) Outer stratifying large dense ganglion cell from lower retina, eccentricity 18.1 mm. Soma diameter was 17 μm. Densely branching dendritic tree was 733 μm in diameter with 148 branch points.

The large dense cells formed a cluster of 21 cells (Fig. 6) and included both inner and outer stratifying cells (Table 1). The dendrites of these cells tended not to cross one another, giving a maze-like appearance to the dendritic tree. The cell in Fig. 7C had the dense, maze-like appearance typical of these cells, though there were a few crossing dendrites in one area of the dendritic tree. Large dense cells had thin axons that typically originated from the soma (arrows in Figs. 7C and 8C) and in only a few cases from a primary dendrite. As with all of the cell groups in this study, large dense cells showed a trend towards increasing dendritic-field size with increasing eccentricity but no trend in soma size with eccentricity (not shown). Unlike the cell groups discussed above, the large dense cells showed a trend towards increasing branch point number with increasing eccentricity (not shown).

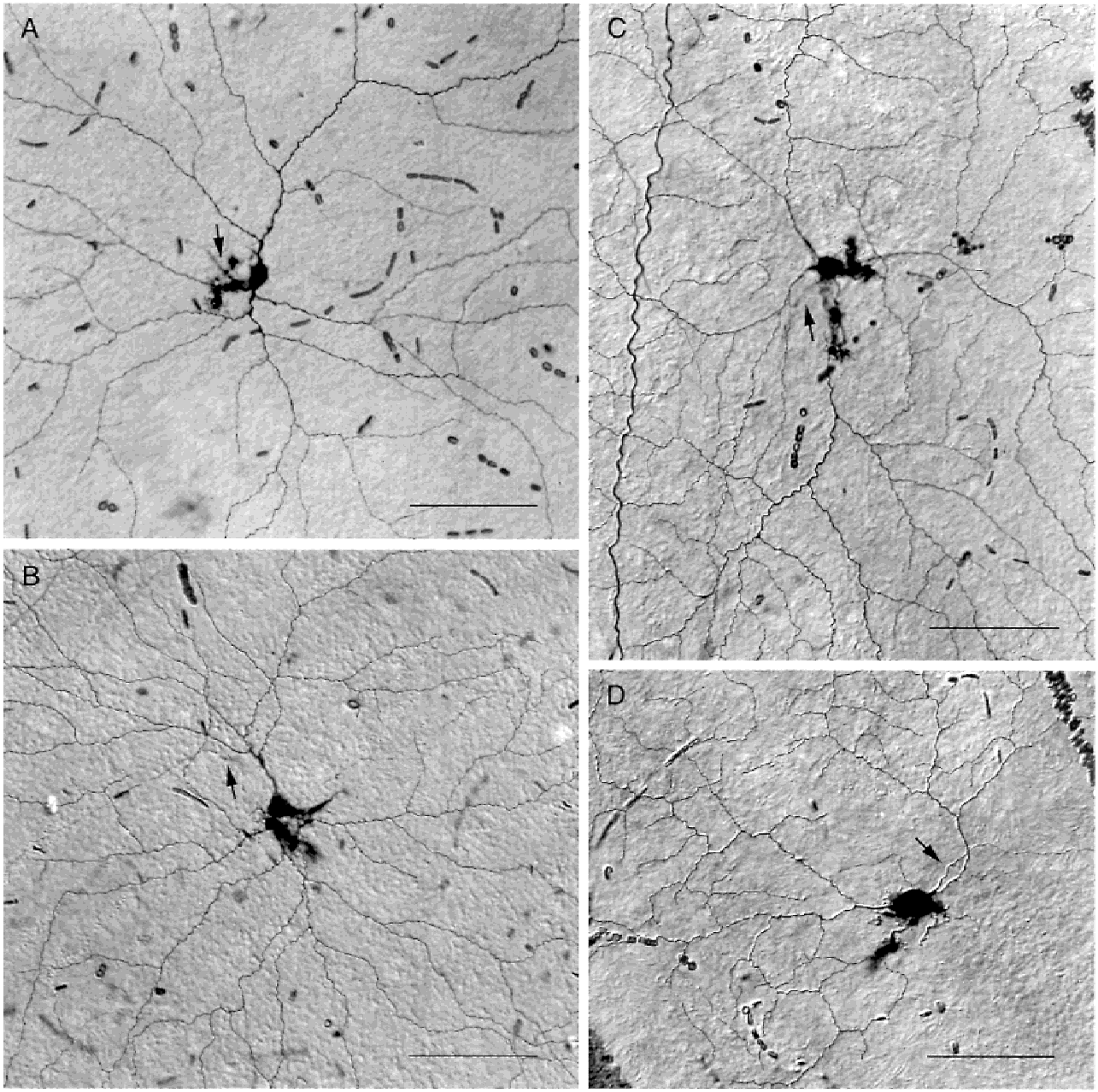

Fig. 8. Photomicrographs of four HRP-filled monostratified ganglion cells. Arrows indicate axons. (A) Inner stratifying large sparse ganglion cell from nasal retina, eccentricity 15.2 mm. Soma was 17 μm in diameter. Dendritic tree was 765 μm in diameter with 50 branch points. (B) Inner stratifying large moderate ganglion cell from upper retina, eccentricity 7.1 mm. A tracing of this cell is shown in Fig. 7B. (C) Inner stratifying large dense ganglion cell from upper retina, eccentricity 13.2 mm. Cell had 120 branch points and a dendritic-field diameter of 755 μm. Soma diameter was 18 μm. (D) Inner stratifying thorny monostratified ganglion cell from temporal retina, eccentricity 10.3 mm. Medium-size dendritic tree was 404 μm in diameter with 80 branch points. Soma diameter was 21 μm. Scale bars = 100 μm.

None of the cells in the large sparse, large moderate, or large dense groups were filled with Neurobiotin so it was not possible to determine if any of these cells were heterotypically or homotypically coupled.

Thorny monostratified ganglion cells

A total of 15 cells had medium-size dendritic trees compared to the large dendritic trees of cells in the other five groups (Table 1). When plotted for branch point number, they overlapped the large sparse and large moderate cell clusters (Fig. 9). All 15 cells were broadly inner stratified. The dendritic morphology of these cells, which we have termed thorny monostratified, was also distinctly different from cells in the other five groups (Figs. 8D and 10). Thorny monostratified cells had thick, very spiny primary dendrites that gave off thin, spiny, secondary branches that in turn had many shorter, very fine, spiny, twig-like branchlets (Fig. 10 inset). The overall appearance was of a thorny tangle of branches (Fig. 10). The cells in the photomicrograph of Fig. 8D and the tracing of Fig. 10 had the retroflexive branching pattern typical of cells in this group, though the thorny appearance of the dendrites is not as apparent in the photomicrograph. Thorny cells had medium size cell bodies (Table 1) with thin axons ($\sim$2 μm) that originated either from the soma (arrow in Fig. 10), or from a primary (arrow in Fig. 8D) or secondary dendrite.

None of the thorny monostratified cells were filled with Neurobiotin. The thorny cells showed a trend towards increasing dendritic-field size and decreasing number of branch points with increasing eccentricity (not shown). The decrease in branch points with eccentricity may reflect a difficulty in filling the finer processes of larger cells.

Others

Five of the wide-field monostratified cells in our sample did not fall into any of the six groups discussed above. One cell, located at an eccentricity of 14 mm, was densely branched (104 branch points) and had an extremely large dendritic tree 1399 μm in diameter. This was the only "giant" dense cell in the sample (not shown).

Four cells had axons that branched within about 100 μm of the cell body. In two of the cells, both axon branches were in the optic fiber layer and ran towards the optic disk. In the other two cells, only one axon branch projected towards the optic disk while the other branch appeared to run in the IPL. We have previously described a type of human retinal ganglion cell with intraretinal axon collaterals that terminate in the IPL (Peterson & Dacey, 1998). The four cells with branching axons in the present study did not exhibit

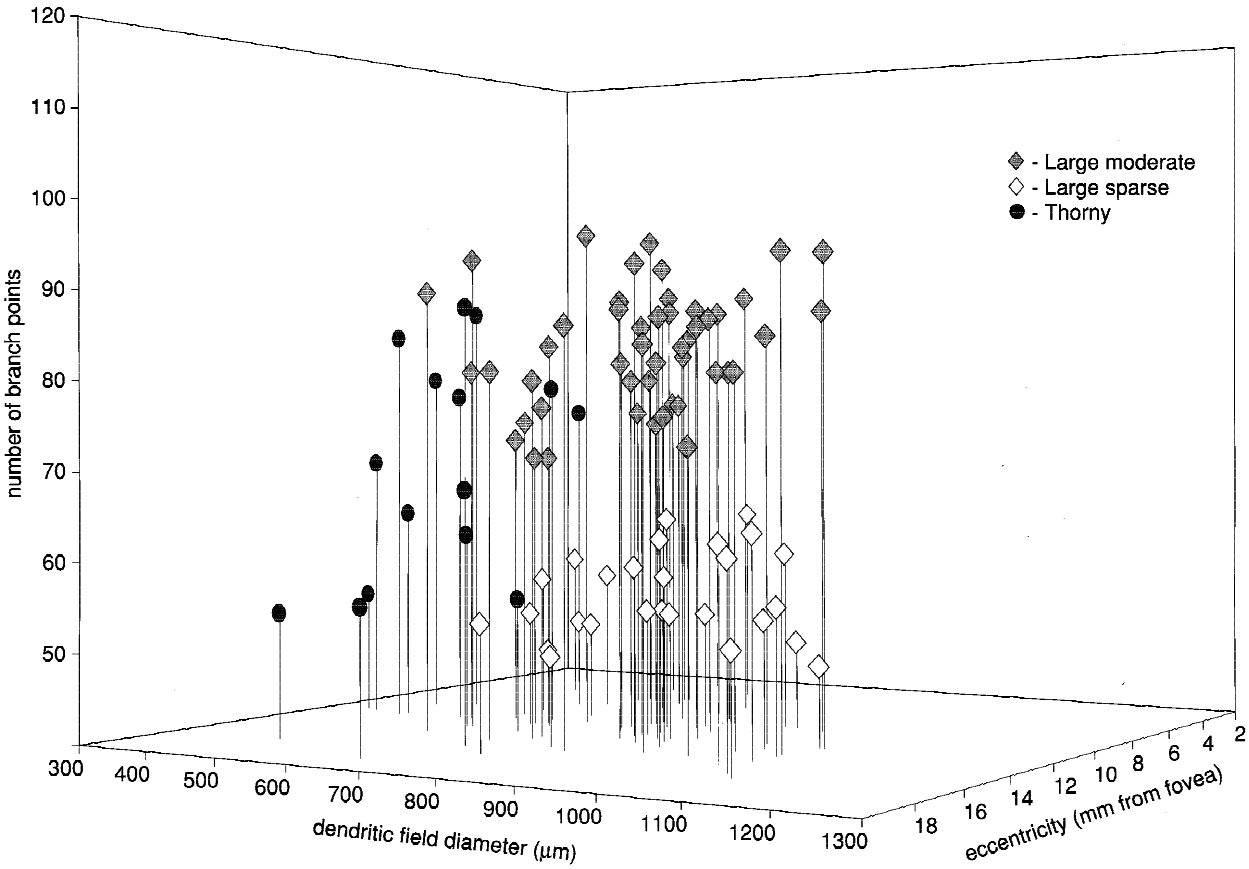

Fig. 9. Three-dimensional scatter plot of wide-field, monostratified ganglion cells. Cells were plotted by number of branch points as a function of dendritic-field diameter and eccentricity. The large sparse and large moderate cells formed clusters distinct from each other. Thorny cells had smaller dendritic fields and overlapped the large sparse and large moderate cells in the number of dendritic branch points.

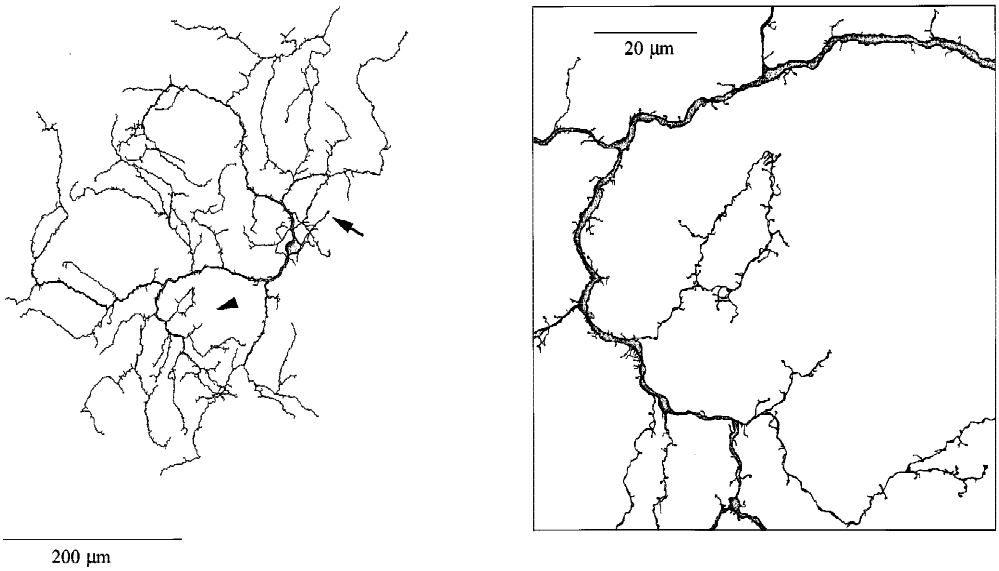

Fig. 10. Camera-lucida tracing of an HRP-filled thorny monostratified ganglion cell from temporal retina, eccentricity 12.2 mm. Arrow indicates axon. Soma diameter was 17 μm, dendritic-field diameter was 424 μm, and the cell had 85 branch points. Arrowhead shows area magnified in the inset to illustrate the thin, spiny branches with short, twig-like branchlets typical of these cells.

the short, thin, varicose terminal collaterals that were a distinctive characteristic of the axon collateral-bearing cells in our previous study. They are similar, however, in dendritic-field size, soma size, and number of dendritic branches. It is always possible that these four cells had terminal collaterals that simply failed to stain. On the other hand, the retina may contain another ganglion cell type or types with branching axons. It is not possible to determine which explanation may account for the ganglion cells with branching axons in the present study based on a sample size of only four cells and without an understanding of their retinal connections or central projections.

Discussion

General remarks

As mentioned above, the wide-field, monostratified cells in the present study came from a larger sample of some 1000 intracellularly injected human retinal ganglion cells. Though ganglion cells were targeted for filling in a random manner, there was a sampling bias towards cells with medium-to-large cell bodies. It is not possible, therefore, to estimate the percentage of human retinal ganglion cells represented by wide-field monostratified cells based on the present study.

Classification

We classified the wide-field, monostratified ganglion cells of the present study into six groups based on measurable morphological characteristics. The six groups are shown together in Fig. 11, which summarizes the human monostratified ganglion cells described here and in previous studies (Dacey & Petersen, 1992; Peterson & Dacey, 1998) and illustrates the differences in dendritic-field size and morphology between midget, parasol, and wide-field cells. It is not possible, based on the present study, to say conclusively whether each group of wide-field cells represents a single morphological type or includes several morphologically similar types. Cells in each of the six groups appeared to be fairly homogeneous, though there was some variability within groups. The large very sparse cells in particular showed differences in the thickness and spiny appearance of the dendrites and may possibly represent more than one cell type. On the other hand, the thorny monostratified cells were remarkably similar, suggesting that they may represent a single type of cell.

Cells similar to those of the present study have been seen in Golgi preparations of human retina (Kolb et al., 1992) and in retrograde labeling studies in macaque following tracer injection into midbrain nuclei and the LGN (Leventhal et al., 1981; Perry & Cowey, 1984; Rodieck & Watanabe, 1993). Although these previous studies lacked information on the cell mosaics and could not unequivocally determine specific cell types, the similarities between cells of the present study and those described using different retinal preparations and experimental approaches allow us to draw some tentative conclusions as to the possible types of wide-field, monostratified ganglion cells present in the primate retina.

Comparison to Golgi studies of human retina

Kolb et al. (1992), using a Golgi preparation of human retina, described two very sparsely branched, inner stratifying ganglion cells with large dendritic fields. Though the cells appeared somewhat similar, the authors thought it likely they represented two different cell types since one of the cells was more sparsely branched and had a larger though incompletely impregnated dendritic tree. We also found two groups of very sparsely branched cells with one group having more sparsely branched and considerably larger dendritic trees (Figs. 3 and 4). It seems likely that the larger, more sparsely branched cell described by Kolb et al. and the giant very sparse cells of the present study may represent the same cell type, and that the other sparsely branched cell with a smaller dendritic

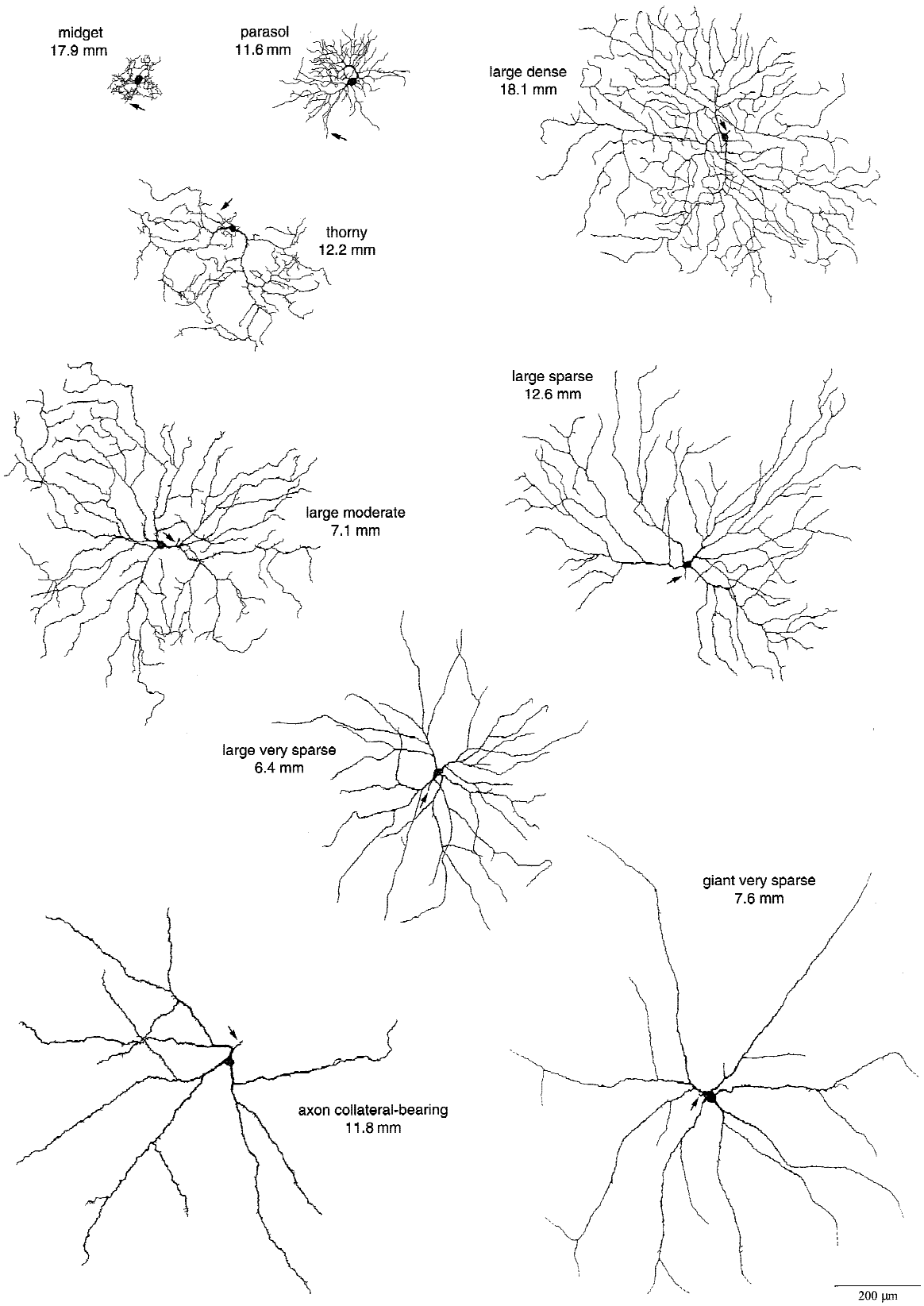

Fig. 11. Comparison of dendritic-field size of HRP-filled midget, parasol, and wide-field monostratified ganglion cells of the human retina. Numbers next to the cells are distances (in mm) from the fovea. The giant very sparse, large very sparse, large moderate, large dense, and thorny cells, are the same as shown in Figs. 4, 7, and 10. The large sparse cell is another example from this group and had a dendritic-field diameter of 785 μm, close to the mean field size for large sparse cells. Axon collateral-bearing cells have been described previously (Peterson & Dacey, 1998) and one is shown here for comparison with the other wide-field cells.

tree described by Kolb et al. may be the same cell type as cells in the large very sparse cell group described here. In the same study, Kolb et al. also described a type of inner stratifying ganglion cell with a medium-size dendritic tree that had many fine and spiny retroflexive dendrites. The Golgi-stained cell was strikingly similar to the thorny monostratified cells in the present study, suggesting that it may be an example of the same cell type.

Comparison to midbrain-projecting macaque monkey cells

Leventhal et al. (1981) identified several classes of ganglion cells that were retrogradely labeled following HRP injections into the pretectum and superior colliculus of macaque monkeys. The labeled cells appeared to have large, sparsely branched dendritic trees, though the authors noted that some of the finer dendrites were not completely filled. Perry and Cowey (1984) also used HRP injections into the superior colliculus and pretectum of macaque monkeys to retrogradely label ganglion cells and found that a heterogeneous group of cells with small- to medium-size cell bodies projects to the midbrain. Though many of the cells in their study were also only partially filled, the majority appeared to have large, sparsely branched dendritic trees. More recently, Rodieck and Watanabe (1993) used intracellular injection of HRP to fill ganglion cells labeled with fluorescent tracer following injections into the pretectum and the superior colliculus of macaque monkeys. Like Leventhal et al. and Perry and Cowey, their results showed that a number of different types of large-field ganglion cells project to the midbrain. Rodieck's and Watanabe's sample of well-filled ganglion cells included several monostratified cell types morphologically similar to cells in the present study and are discussed below.

Among cells found to project to the superior colliculus, Rodieck and Watanabe described a group of large-field ganglion cells they termed maze cells and considered to represent a single type. The maze cells had densely branched dendritic trees very similar to the human large dense cells described here (Fig. 7C). The dendritic-field diameters of human large dense cells were roughly twice that of macaque maze cells. Dendritic-field diameters of human parasol and small bistratified ganglion cells, however, are also larger than their monkey counterparts (Dacey & Petersen, 1992; Dacey, 1993). Despite differences in dendritic-field size, the strikingly similar maze-like morphology of human large dense and macaque maze cells suggests that these cells may be homologous.

Rodieck and Watanabe labeled two types of large, sparsely branched, monostratified ganglion cells following tracer injection into the pretectum. One type, which they termed PT-sparse, closely resembled human giant very sparse cells (Fig. 4A) in the extent and pattern of dendritic branching. The dendritic fields of macaque PT-sparse cells, however, were more similar in size to human large very sparse cells. As noted above, some ganglion cell types differ in dendritic-field diameter in human and monkey retina. Though it cannot be assumed that a difference in size between human and monkey cells would hold true for all types of ganglion cells, the close similarity in the dendritic branching pattern of the human giant very sparse cells and macaque PT-sparse cells suggests that they may be equivalent cell types and that the differences in dendritic-field size may represent a species variation. A larger sample of wide-field, monostratified macaque cells would help to determine whether monkey retina contains ganglion cells similar to both the human giant very sparse and large very sparse cells.

The other type of pretectum-projecting monostratified ganglion cell described by Rodieck and Watanabe was very similar to the human large sparse cells (Fig. 7A) in both the number and pattern of dendritic branching and in dendritic-field size. Rodieck and Watanabe expressed some doubt that this second type actually projected to the pretectum and thought the cells might have been labeled from injected fibers passing through the brachium to the superior colliculus. In an on-going study in our lab of retrogradely labeled ganglion cells, we have confirmed Rodieck's and Watanabe's finding of two types of wide-field, sparsely branched, monostratified ganglion cells projecting to the pretectum in macaque monkeys. Our preliminary results (unpublished) included cells that were morphologically very similar to Rodieck's and Watanabe's second type of pretectum-projecting monkey cell and to the human large sparse cells. We also labeled very sparsely branched macaque cells with large dendritic trees that closely resembled Rodieck's and Watanabe's PT-sparse cells and the human giant very sparse cells.

In summary, morphological similarities between human and macaque cells suggest that the giant very sparse and large sparse groups may represent human correlates of macaque cells shown to project to the pretectum, while the large dense cells may be the human equivalent of macaque cells that project to the superior colliculus.

Comparison to LGN-projecting macaque monkey cells

In another study of retrogradely labeled macaque ganglion cells, Perry et al. (1984) concluded that the vast majority of cells projecting to the magnocellular layers of the LGN were Pα or parasol cells while the majority of parvocellular-projecting cells were Pβ or midget ganglion cells, and that the occurrence of other cell types projecting to these regions was very rare. Their conclusions, however, were based largely on soma size since their method of retrogradely filling ganglion cells with HRP injected into the LGN often failed to reveal the dendritic morphology of labeled cells. It has now been shown that a greater diversity of ganglion cell types projects to the LGN in primates (Rodieck & Watanabe, 1993) and that a third geniculocortical pathway transmits color information to visual cortex *via* the interlaminar zones of the LGN (Hubel & Livingstone, 1990; Hendry & Yoshioka, 1994; Martin et al., 1997).

In their study of midbrain-projecting cells discussed above, Rodieck and Watanabe (1993) also labeled ganglion cells following fluorescent tracer injection into the parvocellular layers of the LGN and were able to recover the full dendritic morphology of a large number of cells. Though most of the labeled cells were midget ganglion cells, Rodieck and Watanabe also described a bistratified cell type and a type of large, monostratified ganglion cell. The monostratified cells, which they termed parvocellular giant, are remarkably similar to the human large moderate cells (Fig. 7B) in the extent and pattern of dendritic branching, and also are similar in dendritic-field size and soma size, suggesting these may be equivalent cell types. Rodieck and Watanabe thought it possible that the sparse population of macaque parvocellular giant cells may project to the interlaminar zones between the parvocellular layers of the LGN, though a precise determination of the target sites of parvocellular giant cells could not be made from the injection site. Further studies of the morphology and physiology of macaque parvocellular giant cells are needed to determine their functional role in visual perception and whether they make any contribution to color pathways.

Acknowledgments

Special thanks to Kim Allen of the Lions Eye Bank, Toni Haun, and Keith Boro for technical help. This work was supported by PHS Grant EY07031 and by NIH Grant EY06678.

References

Boycott, B.B. & Dowling, J.E. (1969). Organization of the primate retina: Light microscopy. *Philosophical Transactions of the Royal Society* (London) **255**, 109–184.

Dacey, D.M., Petersen, M.R. & Allen, K.A. (1991). Beyond the midget and parasol cells of the human retina. *Investigative Ophthalmology and Visual Science* (Suppl.) **32**, 1130.

Dacey, D.M. & Petersen, M.R. (1992). Dendritic field size and morphology of midget and parasol ganglion cells of the human retina. *Proceedings of the National Academy of Sciences of the U.S.A.* **89**, 9666–9670.

Dacey, D.M. (1993). Morphology of a small-field bistratified ganglion cell type in the macaque and human retina. *Visual Neuroscience* **10**, 1081–1098.

Dacey, D.M. & Lee, B.B. (1994). The 'blue-on' opponent pathway in primate retina originates from a distinct bistratified ganglion cell type. *Nature* **367**, 731–735.

Dacey, D.M. (1994). Physiology, morphology and spatial densities of identified ganglion cell types in primate retina. In *Higher Order Processing in the Visual System*, ed. Goode, J. & Morgan, M., pp. 12–34. London: Ciba Foundation Symposium No. 184.

Dacey, D.M. (1996). Circuitry for color coding in the primate retina. *Proceedings of the National Academy of Sciences of the U.S.A.* **93**, 582–588.

Ghosh, K.K., Goodchild, A.K., Sefton, A.E. & Martin, P.R. (1996). Morphology of retinal ganglion cells in a New World monkey, the marmoset *Callithrix jacchus*. *Journal of Comparative Neurology* **366**, 76–92.

Hendry, S.H.C. & Yoshioka, T. (1994). A neurochemically distinct third channel in the macaque dorsal lateral geniculate nucleus. *Science* **264**, 575–577.

Hubel, D.H. & Livingstone, M.S. (1990). Color and contrast sensitivity in the lateral geniculate body and primary visual cortex of the macaque monkey. *Journal of Neuroscience* **10**, 2223–2237.

Kolb, H., Linberg, K.A. & Fisher, S. (1992). Neurons of the human retina: A Golgi study. *Journal of Comparative Neurology* **318**, 147–187.

Leventhal, A.G., Rodieck, R.W. & Dreher, B. (1981). Retinal ganglion cell classes in the Old World monkey: Morphology and central projections. *Science* **213**, 1139–1142.

Leventhal, A.G., Thompson, K.G. & Liu, D. (1993). Retinal ganglion cells within the foveola of New World (*Saimiri sciureus*) and Old World (*Macaca fascicularis*) monkeys. *Journal of Comparative Neurology* **338**, 242–254.

Martin, P.R., White, A.J.R., Goodchild, A.K., Wilder, H.D. & Sefton, A.E. (1997). Evidence that blue-ON cells are part of the third geniculocortical pathway in primates. *European Journal of Neuroscience* **9**, 1536–1541.

Perry, V.H. & Cowey, A. (1984). Retinal ganglion cells that project to the superior colliculus and pretectum in the macaque monkey. *Neuroscience* **12**, 1125–1137.

Perry, V.H., Oehler, R. & Cowey, A. (1984). Retinal ganglion cells that project to the dorsal lateral geniculate nucleus in the macaque monkey. *Neuroscience* **12**, 1101–1123.

Peterson, B.B. & Dacey, D.M. (1998). Morphology of human retinal ganglion cells with intraretinal axon collaterals. *Visual Neuroscience* **15**, 377–387.

Ramon y Cajal, S. (1893). La retina des vertebres. *La Cellule* **9**, 17–257. Translated into English by McGuire, D. & Rodieck, R.W., in *The Vertebrate Retina: Principles of Structure and Function*, San Francisco, California: W.H. Freeman, 1973.

Rodieck, R.W. & Watanabe, M. (1993). Survey of the morphology of macaque retinal ganglion cells that project to the pretectum, superior colliculus, and parvicellular laminae of the lateral geniculate nucleus. *Journal of Comparative Neurology* **338**, 289–303.

Silveira, L.C.L., Yamada, E.S., Perry, V.H. & Picanco-Diniz, C.W. (1994). M and P retinal ganglion cells of diurnal and nocturnal New-World monkeys. *NeuroReport* **5**, 2077–2081.

Watanabe, M. & Rodieck, R.W. (1989). Parasol and midget ganglion cells of the primate retina. *Journal of Comparative Neurology* **289**, 434–454.

Yamada, E.S., Silveira, L.C.L. & Perry, V.H. (1996). Morphology, dendritic field size, somal size, density, and coverage of M and P ganglion cells of dichromatic *Cebus* monkeys. *Visual Neuroscience* **13,** 1011–1029.